Available online at www.sciencedirect.com
SCIENCE DIRECT®
Journal of Chromatography A, 1009 (2003) 15–28
JOURNAL OF CHROMATOGRAPHY A
www.elsevier.com/locate/chroma

Peptide mapping by reversed-phase high-performance liquid chromatography employing silica rod monoliths

Tom P. Hennessy[a], Reinhard I. Boysen[a], Marion I. Huber[b], Klaus K. Unger[b], Milton T.W. Hearn[a,*]

[a]*Australian Research Council Special Research Centre for Green Chemistry, Centre for Bioprocess Technology and Australian Centre for Research on Separation Science, Monash University, P.O. Box 23, Clayton, Victoria 3800, Australia*
[b]*Institut für Analytische Chemie und Anorganische Chemie, Johannes Gutenberg-Universität, Duesbergweg 10–14, 55099 Mainz, Germany*

Abstract

In this paper, a general procedure is described for the generation of peptide maps of proteins with monolithic silica-based columns. The peptide fragments were obtained by tryptic digestion of various cytochrome *c* species with purification of the tryptic fragments achieved by reversed-phase high-performance liquid chromatographic methods. Peak assignment of the various peptides was based on evaluation of the biophysical properties of the individual peptides and via mass spectrometric identification. The performance of several different monolithic sorbents prepared as columns of identical cross-sectional dimensions were investigated as part of these peptide mapping studies and the data evaluated by applying solvent strength theory. These studies revealed curvilinear dependencies in the corresponding relative resolution maps. These findings directly impact on the selection of specific sorbent types or column configurations for peptide separations with silica rod monoliths. Moreover, the influence of variations in the amino acid sequence of the cytochrome *c*s were evaluated with respect to their effect on intrinsic hydrophobicity, the number of experimental observed tryptic cleavage sites, detection limits of the derived fragments in relation to their molecular size, and the chromatographic selectivity and resolution of the various peptides obtained following enzymatic fragmentation of the parent protein. Finally, the scope of these approaches in method development was examined in terms of robustness and efficiency.

Keywords: Monolithic columns; Peak assignment; Solvent strength theory; Resolution maps; Molten globular state; Binding domains; Peptides; Cytochromes

1. Introduction

Reversed-phase high-performance liquid chromatography (RP-HPLC) procedures dominate the analysis and purification of biological molecules as a result of the high level of reproducibility, selectivity and sensitivity that can be achieved [1–6]. The ability of RP-HPLC methods to monitor subtle changes in the biophysical properties [7–11] of peptides and proteins is commonly exploited by taking advantage of the complex equilibria that peptides and proteins undergo in these non-polar ligand systems [11–22]. Theoretical models, based

*Corresponding author. Tel.: +61-3-9905-3720; fax: +61-3-9905-5882.
E-mail address: milton.hearn@med.monash.edu.au (M.T.W. Hearn).

0021-9673/03/$ – see front matter
doi:10.1016/S0021-9673(03)00445-X

on unified concepts of hydrophobicity, bonding theory, solvolysis and the structure of condensed matter [5,10,23] are increasingly being employed to describe these phenomena in considerable molecular detail and to provide insight into the underlying interaction mechanisms that dictate the selectivity and peak efficiencies associated with the separation of peptides and proteins with RP-HPLC systems.

Recently, monolithic silica-based sorbents in polyether ether ketone (PEEK) columns have been introduced [24–30]. These packing materials contain a bimodal pore structure that significantly reduces the column back pressure, thus offering the options of high flow-rates, dramatic reductions in separation time and significantly increased sample throughput. The presence of macropores, forming a dense network of pores around the silica skeleton, as part of these monolithic sorbents allows rapid transit of the eluent through the chromatographic bed, whilst the presence of mesopores creates a large surface area for selective adsorption of the analytes. Silica rod monoliths with bimodal pore structures have already been evaluated in separations of a variety of organic compounds, low-molecular-mass biomolecules and pharmaceuticals, but have yet to be extensively applied as reversed-phase systems in the structural peptide mapping analysis of proteins [31].

In terms of current concepts about peptide (or protein)–non-polar ligand interactions, it is now recognised that the retention behaviour of these biomolecules with RP-HPLC sorbents involves dominant contributions from specific contact regions rather than the total molecular surface of the solute. Moreover, experimental data indicate that peptides and proteins interact with the chromatographic surface in an orientation-specific manner [19,21,32,33]. Both kinetic as well as equilibrium thermodynamic processes contribute to the interactive behaviour that is established between the peptide (or protein), the mobile phase and the stationary phase and thus to the observed retention and peak shape [32,34,35]. The retention properties of peptides and proteins with traditional microparticulate, macroporous *n*-alkylsilica sorbents are determined globally inter alia by their intrinsic hydrophobicity and charge state, but at the molecular level by the nature of specific amino acid residues in contact with the surface of the reversed-phase sorbents rather than by the entire amino acid sequence. The precise locations of these chromatographic contact regions in many cases are not readily predicted. However, molecular foot-printing procedures developed in this laboratory utilising inter alia proteolytic techniques to identify regions of a protein adsorbed in the monolayer state to the non-polar surface provide some insight into the molecule characteristics of these contact regions [5,8,10,32]. Because of the morphological as well as ligand distribution differences of silica rod monolithic sorbents, we were motivated, in the present studies, to examine the selective behaviour of several different silica rod monolithic reversed-phase sorbents manufactured as columns of different dimensions with tryptic peptides derived from protein homologues. These studies, in particular, permitted the performance features of these new sorbents to be documented for closely related peptide sequences as well as protocols to be established that should be of general application in the structural analysis of proteins via enzymatic or chemical mapping methods.

2. Experimental

2.1. Chemicals and reagents

Acetonitrile (HPLC grade) was obtained from Biolab Scientific (Sydney, Australia). Water was distilled and deionised in a Milli-Q system (Millipore, Bedford, MA, USA). Trifluoroacetic acid (TFA) was obtained from Auspep (Melbourne, Australia). The cytochrome *c* species (equine, bovine, canine, avian all from the respective hearts) were obtained from Sigma (St. Louis, MO, USA) and were used without further purification. Trypsin was purchased from Worthington (Freehold, NY, USA). Ammonium hydrogencarbonate was obtained from Mallinckrodt (Paris, KY, USA). Acetone and calcium chloride were from BDH (Kilsyth, Australia). Unless otherwise stated, all solvents and other chemical reagents were of analytical grade.

2.2. Apparatus

Preliminary chromatographic separations were performed on a Waters Associates (Milford, MA, USA) Liquid Chromatograph 484 system consisting of a Waters binary pump, a Waters 484 tunable

absorbance detector, a Waters 712 WISP autosampler, and a Waters 600-MS system controller with the total system controlled by Millenium operating software. Chromatographic analyses were carried out with a Waters Breeze system comprising a Waters 1525 binary pump, a Waters 2487 dual-wavelength absorbance detector, and a Rheodyne manual injector controlled using the Breeze software (except for the manual injector).

2.3. Experimental procedures

2.3.1. Tryptic cleavage of cytochrome c in solution

Cytochrome *c* of various species was incubated with [(L-tosylamido-2-phenyl)ethylchloromethylketone] (TPCK)-treated trypsin in the cleavage buffer (50 m*M* ammonium hydrogencarbonate, 2 m*M* calcium chloride) with continuous agitation. TPCK was used to inhibit any contaminating chymotryptic activity. Based on the calculation of the total number of accessible cleavage sites within the protein, trypsin was employed at a protein:trypsin ratio of 20:1. The cleavage process was stopped after 24 h with the addition of 25 μl of 5 *M* HCl. Free solution incubations of the proteins were also performed using cleavage buffer without trypsin. In addition, trypsin was incubated in cleavage buffer in absence of the cytochrome *c* proteins, under the same conditions as for the analysis of the free solution digests of the cytochrome *c* species in order to distinguish cytochrome *c* fragments from peptide fragments derived from the autocatalytic self digestion of trypsin. All concentrations were adjusted to 1 mg/ml in relation to protein content. Trypsin was dissolved in the cleavage buffer and added to the protein as a stock solution to achieve the desired protein:trypsin ratio.

2.3.2. Instrumental methods for peptide map analyses

The crude peptide digests were separated by gradient elution RP-HPLC using a Waters Breeze HPLC system with either Chromolith Performance RP 18e (100×4.6 mm, lot No. Fr 440 with average macropores of 2000 nm and mesopores of 13 nm), Chromolith SpeedROD RP-18e (50×4.6 mm; lot No. Fr 369 with average macropores of 2500 nm and mesopores of 25 nm) or Chromolith SpeedROD RP-18e (100×4.6 mm; lot No. Fr 369 with average macropores of 2500 nm and mesopores of 25 nm) columns, respectively, containing monolithic, *n*-octadecylsilicas. The eluents employed were A: 0.1% TFA in water and B: 0.09% TFA in acetonitrile–water (60:40, v/v), with a linear gradient of 5–60% B (or 5–50% B for the SpeedROD RP-18e) over times varying from 5 to 60 min, respectively, as detailed below. Bulk solvents were filtered and degassed by sparging with helium. UV detection was employed at 214 nm. The flow-rates used were ≤4 ml/min for the Chromolith Performance RP-18e (100×4.6 mm) and ≤8 ml/min for the Chromolith SpeedROD RP-18e columns, respectively. All columns were operated under the so-called borderline back-pressure conditions [36] with continuous monitoring of the back pressure of the complete system [37]. All experiments were carried out at ambient temperatures. All data points were derived from at least duplicate measurements with retention times between replicates varying typically by less than 1%. The column dead volume was measured as the retention time of the non-interactive solute, thiourea. The statistical analysis involved the Sigmaplot 4.01 program (Jandel Scientific) linear and non-linear regression analysis. In all figures presented, the standard deviations of replicates were smaller than the size of the data points shown.

The molecular masses of the purified peptides were confirmed by electrospray ionisation mass spectrometry (ESI-MS) using a Micromass platform (II) quadrupole MS system with an electrospray source with Masslynx NT Ver. 3.2 software (Micromass, Cheshire, UK). The purified peptides in acetonitrile–water (50:50, v/v), with 3% (v/v) formic acid were infused into the instrument at a speed of 10 μl/min. The ESI-MS spectra of the peptide fragments were acquired at 343 K at a cone voltage of 25–60 V over the mass/charge (*m*/*z*) range of 200–2000 u at 70–80 °C.

3. Results and discussion

3.1. Preliminary screening chromatographic separations

Initially, screening experiments were performed to establish the effect on peptide resolution of changes in gradient steepness and the viscous/frictional

resistance of the different silica rod monolith columns with a range of the mobile phase compositions and flow-rates starting from 1 ml/min with a shallow gradient slope (i.e., 1%/min increase in buffer B). These conditions, typical of protocols [2] used in tryptic mapping studies with conventional analytical RP-HPLC columns of 100×4.7 mm I.D. packed with porous, microparticulate sorbents of 5–10 μm particle diameter sorbents, were employed to provide preliminary baseline information on the performance capabilities of the monolithic stationary phases. Evaluation of these parameters, followed by additional experiments with the linear flow velocity progressively increased and the gradient slope adjusted accordingly enabled examination of the retention behaviour of the different parent proteins (Fig. 1). As evident from these results, the chromatographic profiles obtained under the same conditions exhibited good efficiency, with small but reproducible differences in retention times between the different cytochrome *c*s. As noted subsequently, evaluation of the extent of tryptic digestion of the various cytochrome *c*s (as shown in Figs. 2–4) revealed the existence of satellite peaks in close proximity to some of the main peaks, consistent with several of the cleavage sites within these proteins being proximal to each other in the amino acid sequence (such as ...LysLys... or ...LysXaaLys...). Trypsin cleaves at the carboxyl side of Lys and Arg residues and is active [37] between pH 7.0 and pH 9.0. These satellite fractions were collected and analysed via ESI-MS, confirming the presence of tryptic fragments derived from cleavage at both of Lys residues of such LysLys or LysXaaLys motifs with the generation of two peptides, one of which is the C-terminal extended version of the other (by an additional Lys, LysXaa or XaaLys). The presence of double Lys residues within the sequence of the cytochrome *c*s (or for that matter when it occurs in other proteins) thus results in more complex cleavage pattern for the tryptic map due to kinetic reasons. Trypsin also has difficulties to cleave at Arg/Lys residues flanked by Pro/Asp/Glu/cysteine residues [37], reflecting the sensitivity of the enzyme to the local sequence environment. In addition, His in position Xaa within a sequence containing ...LysXaaLys... constitutes another slow cleavage site.

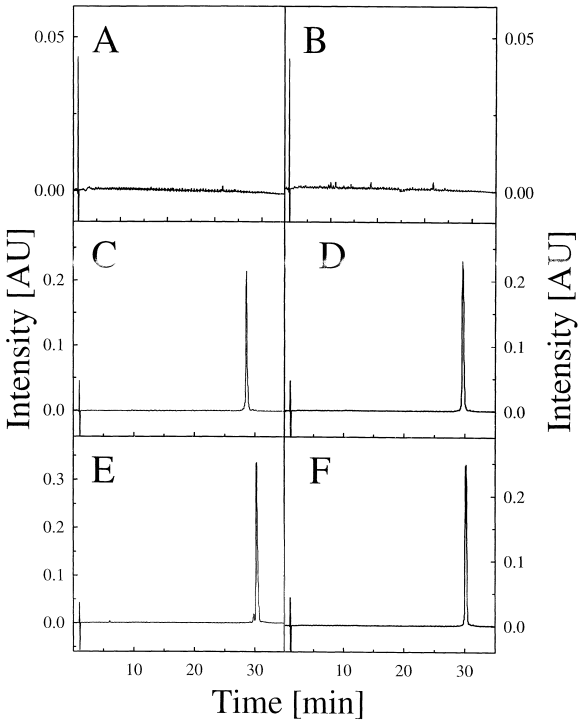

Fig. 1. RP-HPLC separation of (A) cleavage buffer, (B) autolytic trypsin fragments, (C) equine cytochrome *c*, (D) bovine cytochrome *c*, (E) canine cytochrome *c* and (F) avian cytochrome *c* on Chromolith Performance RP-18e. See Experimental section for other details. The code for peptide assignment within the various chromatograms shown as figures 2, 3, 4 and 7 can be identified as follows: (i) the numbers 1, 2, 3, ... correspond to peptides of identical amino acid sequences derived from different cytochrome *c* species according to their elution order (based on the tryptic digest of equine cytochrome *c*); (ii) mutation resulting in no change in retention time for the specified peptide in the chromatogram are shown as ♣; (iii) mutation resulting in variation of the retention time but no change in retention order are shown as ♦; (iv) mutation resulting in variation of both retention time and change in the elution order are shown as ♥.

3.2. Peak assignment of the separated tryptic peptides

Following the preliminary screening investigations described above, it was apparent that the analytical potential of these reversed-phase silica rod monolithic columns could be usefully exploited by coupling them to the low dwell volume instrumental systems (such as 0.4 ml for the Waters Breeze HPLC system compared to 4.5 ml for the Waters Associates Liquid Chromatograph 484 system with 712 WISP

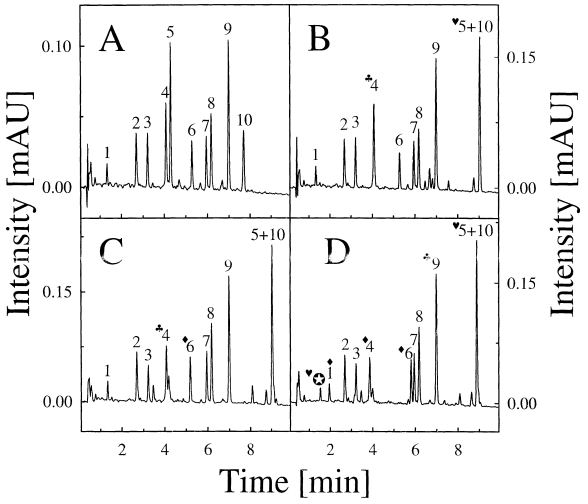

Fig. 2. RP-HPLC separation of tryptic peptide fragments on Chromolith Performance RP-18e of (A) equine cytochrome *c*, (B) bovine cytochrome *c*, (C) canine cytochrome *c* and (D) avian cytochrome *c* at a gradient run time of 10 min. ✪ denotes an additional peak in avian cytochrome *c*. See Experimental section for other details.

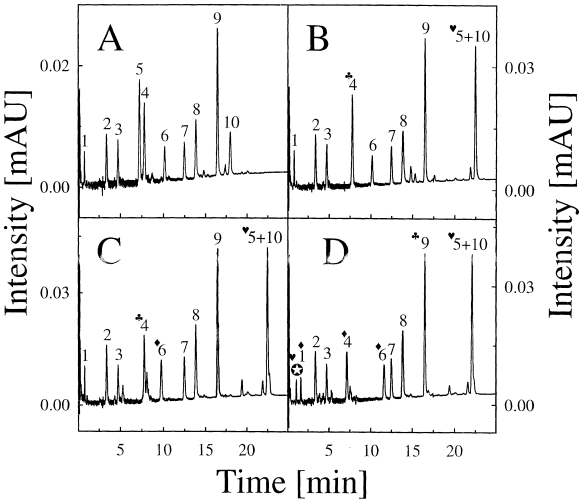

Fig. 4. RP-HPLC separation of tryptic peptide fragments on Chromolith SpeedROD RP-18e 100 mm of (A) equine cytochrome *c*, (B) bovine cytochrome *c*, (C) canine cytochrome *c* and (D) avian cytochrome *c* at a gradient run time of 25 min. See Experimental section for other details.

autosampler) and optimising the gradient separation conditions according to solvent strength theory within the operational limits of the system. Method development and elution order determination with the Chromolith Performance RP-18e column was based on established peak tracking procedures [2,38,39] and were initially applied to the equine cytochrome *c* peptide fragments and subsequently to the peptide digests of bovine, canine and avian cytochrome *c* respectively. As is apparent from Fig. 2A, excellent resolution of the tryptic peptides (numbered according to their elution order) of equine cytochrome *c* was achieved within a 6 min elution window. The sequences of these and the corresponding tryptic peptide fragments derived from the various other cytochrome *c*s are listed in Table 1 and were confirmed by ESI-MS techniques. High reproducibility was also obtained for the separation of the tryptic peptides with identical amino acid sequences but derived from these different protein homologues (Fig. 2A–D) with sequence mutations readily identified when compared with, e.g., equine cytochrome *c*. The impact of amino acid sequence changes on the chromatographic profiles was thus easily monitored.

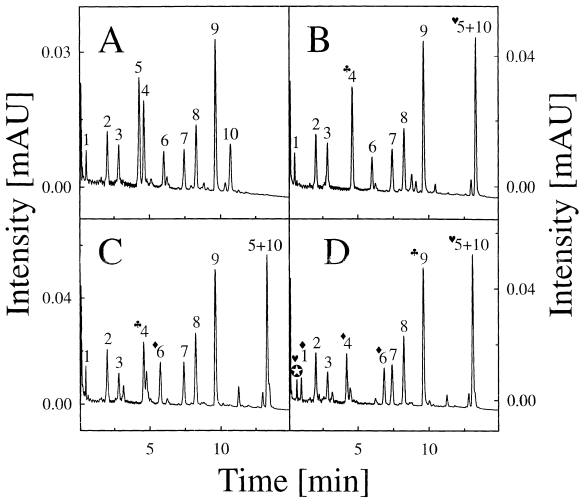

Fig. 3. RP-HPLC separation of tryptic peptide fragments on Chromolith SpeedROD RP-18e 50 mm of (A) equine cytochrome *c*, (B) bovine cytochrome *c*, (C) canine cytochrome *c* and (D) avian cytochrome *c* at a gradient run time of 15 min. See Experimental section for other details.

Although the conformational flexibility exhibited by peptides precludes an unequivocal ab initio determination of the elution order based solely on knowledge of the amino acid sequence and application of hydrophobic fragmental constants or other

Table 1
Tryptic peptide fragments of equine (equ), bovine (bov), canine (can) and avian (avi) cytochrome *c*

Peak	Tryptic fragment	Sequence position	Species	Amino acid sequence	M_r	Hydrophobicity
1	T1	1–5	equ/bov/can	G**D**VEK	588.6	−0.12
1	T1	1–5	avian	GD***I***EK	602.6	1.77
	T2	6–7	all	GK	203.2	−1.41
	T3	8	all	K	146.2	−1.62
3	T4	9–13	all	IFVQK	633.8	8.56
9	T5	14–22	equ/bov/can	C$^{\alpha}$**A**QC$^{\alpha}$HTVEK	1016.2	−0.37
9	T5	14–22	avian	C$^{\alpha}$***S***QC$^{\alpha}$**H**TV**E**K	1032.2	−1.05
	T6	23–25	all	G**G**K	260.3	−1.20
	T7	26–27	all	H**K**	283.3	−3.86
8	T8	28–38	all	TGPNL**H**GLFGR	1168.3	10.95
	T9	39	all	**K**	146.2	−1.62
4	T10	40–53	equine	TGQA**P**GFTY**TD**ANK	1470.6	8.63
4	T10	40–53	bov/can	TGQA**P**GF***S***YTDANK	1456.5	7.36
4	T10	40–53	avian	TGQA***E***GF***S***Y**TD**ANK	1488.5	6.55
	T11	54–55	all	NK	260.3	−1.37
5	T12	56–60	equine	GITWK	603.7	5.01
10	T13	61–72	equine	EETLMEYLENPK	1495.7	8.69
5+10	T12+13	56–72	bov/can	GITW***G***EE**T**LMEYLENPK	2010.3	15.53
5+10	T12+13	56–72	avian	GITW**G**E***D***TLMEY**L**ENPK	1996.2	15.43
	T14	73	all	K	146.2	−1.62
2	T15	74–79	all	YIPGTK	677.8	5.32
7	T16	80–86	all	MIFAGIK	779.0	10.62
	T17	87	all	K	146.2	−1.62
	T18	88	equ/bov/avi	K	146.2	−1.62
	T19	89–91	equine	TER	404.4	−0.30
	T19	89–91	bovine	***G***ER	360.4	−0.30
	T19	89–91	avian	***S***ER	390.4	−1.57
	T18+19	88–91	canine	***TG***ER	461.5	−0.09
6	T20	92–99	equ/bov	ED**L**IAYL**K**	964.1	10.51
6	T20	92–99	canine	***A***D**L**IAYL**K**	906.1	10.67
6	T20	92–99	avian	***V***D**L**IAYL**K**	934.1	12.20
	T21	100	all	K	146.2	−1.62
	T22	101–104	equ/bov	ATNE	433.4	0.86
	T22	101–103	canine	AT***K***	318.4	−0.91
	T23	104	canine	E	147.1	−0.10
✪	T21+22	100–104	avian	***D***AT***SK***	520.5	−1.73
–	heme	–		–	608.35	n.a.
9	T5heme	14–22	equine	C$^{\alpha}$AQC$^{\alpha}$HTVE**K**	1624.5	n.a.

Peak No. according to elution order in the RP-HPLC profiles (cf. Fig. 2A), theoretical tryptic fragments designated as T1, T2, ...T23; amino acid sequence difference for the respective cytochrome *c*s have the specific amino acid(s) highlighted in bold italics; theoretical mass is in Daltons and total hydrophobicity was calculated according to Wilce et al. [40]. These and additional data on the topic can be compiled from http://www.embl-heidelberg.de. The detectable fragments are given in bold and variations in the sequence (relative to equine cytochrome *c*) are italicised. The results are discussed on the basis of the elution order of equine cytochrome *c* fragments shown in Fig. 2A. This procedure requires an additional nomenclature for the tryptic peptides but this is beneficial as changes in the retention behaviour can be identified instantaneously.

molecular descriptor parameters, the retention, once it is established, can be described in terms of the biophysical properties of the peptides and the framework of solvent strength theory. Variations in column properties result in predictable differences of elution behaviour, whilst the effects of changes in the amino acid sequence or the site of cleavage can be rationalised by utilising existing knowledge on the physicochemical properties of the particular amino acids in question.

Previously, hydrophobicity coefficients [22,40] have been used to predict the relative retention times of the various peptides in RP-HPLC systems and thus their elution order. Employment of these coefficients, in principle, enables the prediction of the elution order of the parent cytochrome *c* proteins under the experimental conditions of the screening chromatographic separations as well as the elution order of the major tryptic fragments (as detailed below) after digestion. Application of these procedures based on the C_{18}-scale of Wilce et al. [40] generally resulted in the predicted retention times being in good agreement with the experimental observations. In the case of the cytochrome *c* proteins the observed order followed these predictions with the order of elution found to be equine, bovine, avian and canine cytochrome *c*, respectively (the latter having an identical amino acid sequence as equine cytochrome *c* for the respective peptide T5+T10). However, for the tryptic peptides, the hydrophobic properties of the peptides T5, T9 and T10 (Table 1) appear to have been over emphasised in these predictions. For the cytochrome *c*s, the amino acid sequences corresponding to the peptide fragments T5 and T10, i.e., the amino acid sequence residues Gly^{56} and Lys^{72} respectively, have been determined by molecular foot-printing experiments [2,5,32,41] to participate in the contact region of equine cytochrome *c* when this protein is adsorbed to *n*-butylsilicas.

With these silica rod monolithic reversed-phase columns, peptide T10 was retained longer than any other equine cytochrome *c* peptide fragment, which is contradictory to its predicted retention behaviour based on a random coil structure and the summated hydrophobicity coefficients of the amino acid sequence. The presence of an amphipathic secondary structure for peptide T10 is required under these reversed-phase conditions if a high correlation is to be obtained between the predicted and observed retention time for this peptide. Anticipation of sequence regions corresponding to the contact sites of polypeptides or proteins in association with chromatographic sorbents cannot generally be made solely from knowledge of the hydrophobicity of the amino acid residue sequence. From the X-ray crystallographic data available [42] for equine cytochrome *c*, the amino acid sequence corresponding to peptide T10 predominantly exists in an α-helical conformation. Moreover, peptide T10 exhibits a retention time very similar to the parent protein, whilst molecular foot-printing experiments have indicated that the amino acid sequence corresponding to this peptide fragment plays a significant role in the retention of the non-digested protein. These findings have been previously interpreted as evidence for the peptide T10 sequence acting as a key contributor to the hydrophobic binding domain of equine cytochrome *c*. The conclusion can be drawn from these results that upon enzymatic fragmentation and on binding to the *n*-octadecyl ligands present at the surface of these silica rod monoliths, rather than undergoing an α-helix→random coil transition, the amino acid sequence corresponding to peptide T10 of equine cytochrome *c* adopts or maintains a partial α-helical structure with juxtapositioning of the non-polar side chains leading to the observed retention behaviour.

Other studies [5,8,43] are consistent with this interpretation. In particular, circular dichroism (CD) spectroscopic investigations indicate increased helicity of cytochrome *c* in acetonitrile water mixtures as compared to physiological conditions. In contrast, the amino acid sequence corresponding to peptide T5 in equine cytochrome *c* in the crystalline state does not display any significant secondary structural features. When compared to the other peptide fragments, e.g., peptide T3, peptide T5 contains a larger number of less hydrophobic amino acids with the Ile^{57} and Trp^{59} residues displaced by Thr^{58} with the peptide overall having a lower propensity to adopt a secondary structure. For peptide T3 the Ile^{9} residue is adjacent to Phe^{10} and thus a more restricted access to the hydrophobic binding site may arise due to the adjacent presence of the Val^{11}, Gln^{12} and Lys^{13} residues. The observed shift towards later elution than predicted for peptide T9 can be explained due to the covalent attachment of the heme group, which is not accommodated in the available hydrophobicity scales, to the cysteine residues at positions Cys^{14} and Cys^{17} in the amino acid sequence.

Several biophysical properties of the tryptic peptides derived from the various cytochrome *c*s (equine, bovine, canine, avian) are summarised in Tables 1–3. For all of the cytochrome *c*s peptide fragments T2, T3, T7 and T8 have the same amino

Table 2
Extent of molecular diversity in terms of amino acid substitutions of various cytochrome *c* species relative to equine and canine cytochrome *c*, compiled from http://www.embl-heidelberg.de

	Canine	Avian	Bovine	Equine
Canine	–	10	3	6
Avian	10	–	9	11
Bovine	3	9	–	3
Equine	6	11	3	–

acid sequences and thus have unchanged retention times in all chromatograms. Equine cytochrome *c* contains a Lys residue at position 60. Since none of the other cytochrome *c*s contain this particular cleavage site, a tryptic fragment denoted by peptide T5+T10 and encompassing the amino acid residues 56–60 and 61–72 is generated and elutes as a single peak. As is apparent from Table 2, the extent of molecular diversity compared to the equine cytochrome *c* sequence increases in the order bovine, canine and avian cytochrome *c*. The conserved substitution of Thr^{47} in the peptide T4 of equine cytochrome *c* for Ser^{47} in bovine cytochrome *c* does not result in a changed retention time (cf. Fig. 2A and B). In terms of resolution of the Thr^{47}-mutant peptide T4 from the Ser^{47}-peptide T4, this RP-HPLC system is thus insensitive to this particular amino acid substitution.

Compared to equine cytochrome *c*, the sequence of canine cytochrome *c* varies at six locations, resulting in the corresponding peptide T4 with unchanged retention time, peptide T6 with a shift towards earlier elution and the peptide T5+T10 with variation in the elution profile, respectively (Fig. 2C). The retention behaviour of canine peptide T6 deserves more detailed examination, since the difference in hydrophobicity induced through the substitution ($Glu^{92}\rightarrow Ala^{92}$) suggests later elution of this peptide. With this substitution occurring at the N-terminal end of this peptide it can be concluded that the introduction of Ala^{92} significantly affects the binding this peptide to the *n*-alkyl moieties on the monolithic silica, i.e., reduces the contact area of the retained peptide and hence leads to the observed shorter elution time of this tryptic fragment compared to the other peptides. Due to the detection limit with peptide fragments of <5 amino acid residues lacking a UV-absorbing chromophore, i.e., the single Lys (as the amino acid) cleaved from positions 8, 39, 73, 87 or 88, and the di-, tri- or tetrapeptide fragments, UV detection at 214 nm fails to monitor these fragments (or their sequence variations across the other cytochrome *c* species, derived from, e.g., the canine cytochrome *c*s (cf. Fig. 1C), with these fragments eluting at or near the void volume of the column as assessed from ESI-MS studies.

Similar considerations apply to the UV detection at 214 nm of 10 out of 11 sequence variations in the map of avian cytochrome *c* (Fig. 2D). The appearance of the peptide fragment, designated in Fig. 2D as peptide ✪, is the result of a deleted cleavage site at residue position 100, resulting in the generation of a single peptide fragment (peptide T21+T22). The peptide fragment corresponding to the sequence of peak ✪ contains several polar amino acids and thus it is not surprising that the peptide ✪ elutes at the very beginning of the chromatogram (the gradient starting condition with 5% ACN could be successfully used to retain peptide ✪ on the various columns under isocratic conditions). As evident from a comparison of Fig. 2A and D, the substitute of $Val^{3}\rightarrow Ile^{3}$ results in the later elution of the corresponding avian

Table 3
Location and characteristics of the distinguishing amino acids from four cytochrome *c* species, compiled from http://www.embl-heidelberg.de, non depicted amino acid residues are identical

Species	Sequence position number and nature of amino acid substitution											
	3	15	44	47	60	62	88	89	92	100	103	104
Equine	Val	Ala	Pro	Thr	Lys	Glu	Lys	Thr	Glu	Lys	Asn	Glu
Bovine	Val	Ala	Pro	Ser	Gly	Glu	Lys	Gly	Glu	Lys	Asn	Glu
Canine	Val	Ala	Pro	Ser	Gly	Glu	Thr	Gly	Ala	Lys	Lys	Glu
Avian	Ile	Ser	Glu	Ser	Gly	Asp	Lys	Ser	Val	Asp	Ser	Lys

All 12 listed variable amino acid residues are to some extent surface exposed, as found from corresponding three-dimensional structures.

peptide T1, which is in good agreement with the expected effect of this replacement in terms of the hydrophobicity of the fragment.

Peptide T4 of avian cytochrome *c* comprises the null retention-change $Ser^{47} \rightarrow Thr^{47}$ substitution apparent with the bovine and canine species. The observed peak of faster elution can therefore be assigned to the substitution of Pro^{44} by Glu^{44}. With regard to the longer retained peptide T6 of avian cytochrome *c*, this effect again can be readily interpreted in terms of the single $Glu^{92} \rightarrow Val^{92}$ substitution. The inter-species variation in the elution position of peptide T9 of avian cytochrome *c* (when compared to the corresponding peptide derived from the equine, bovine or canine species) is consistent with the amino acid substitution at position 15 ($Ala^{15} \rightarrow Ser^{15}$) with attendant decrease in hydrophobicity and faster elution of the fragment. The observed behaviour, however, supports the assumption that the attached heme group (evidence for the covalent attachment of the heme group to this peptide fragment was gained from the ESI-MS spectrum of this fragment) governs the chromatography of this fragment and moreover that the sequence position at which the residue variation occurs is not involved in the binding domain.

Compared to equine cytochrome *c*, the amino acid sequence corresponding to the peptide T10 in avian cytochrome *c* contains two substitutions. Substitution of Lys^{60} by Gly^{60}, again, leads to the abolition of the tryptic cleavage site (and the generation of the combination peptide T5 + T10 fragment in the corresponding peptide map of avian cytochrome *c*). On the other hand, the substitution of Glu^{62} by Asp^{62} in avian cytochrome *c* leads to the formation of the peptide T5 + T10 fragment that elutes slightly faster than the corresponding peptide T5 + T10 fragment of bovine or canine cytochrome *c*. Since the $Glu^{62} \rightarrow Asp^{62}$ substitution involves only a net removal of a CH_2 group in a relatively large peptide fragment, it is apparent that these monolithic systems, in common with the more traditional microparticulate *n*-alkylsilica sorbents, can be responsive to very minor changes in composition of peptides provided the modification is involved in the molecular contact site for interaction with the *n*-alkyl ligand.

In these studies, hydrophobicity coefficients and chromatographic profiles have been utilised as complementary tools to evaluate the molecular basis of tryptic peptide and parental protein retention with these monolithic sorbents and specifically the nature of the molecular binding domain examined from a comparison of the bovine and canine cytochrome *c* homologues, which vary in 3 out of 104 amino acid residues (bovine cytochrome *c*: Lys^{88}, Glu^{92}, Asn^{103}/canine cytochrome *c*: Thr^{88}, Ala^{92}, Lys^{103}, cf. Tables 2 and 3). Upon digestion the fragments that contribute to the molecular contact site with the sorbent display equal hydrophobicity coefficients and retention times, whereas peptide T6 of bovine elutes after the canine species. Summation of the hydrophobicity coefficients for the parent proteins predicted the elution of bovine ahead of canine cytochrome *c*, which was readily confirmed experimentally. Hence, amino acid residues at positions 88 and 92 can be assigned to form part of the binding domain of the parent protein, despite the absence of spectroscopic techniques that can accurately determine the orientation of proteins upon adsorption to reversed-phase (monolithic) sorbents.

3.3. Evaluation of the different monolithic columns

With the establishment of the elution order via peak assignment with the Chromolith Performance RP-18e columns, similar procedures were repeatedly applied to all columns under investigation. The results are shown in Fig. 3 for the SpeedROD 50 mm column and Fig. 4 for the SpeedROD 100 mm column. The most evident difference between the Chromolith Performance RP-18e column and the SpeedROD 50 mm or SpeedROD 100 mm columns is the pore size. The wide pore monoliths can be operated at twice the flow-rate as compared to the Chromolith Performance RP-18e column at the cost of decreased capacity and possibly selectivity due to loss of surface area. Consequently, the SpeedROD 50 mm or SpeedROD 100 mm columns were operated with a more shallow gradient (for details see the Experimental section). Under such conditions, high resolution, rapid separations of the peptide digests could also be achieved with these larger pore monolith columns as apparent from a comparison of the corresponding results shown in Fig. 2 with Figs. 3 and 4.

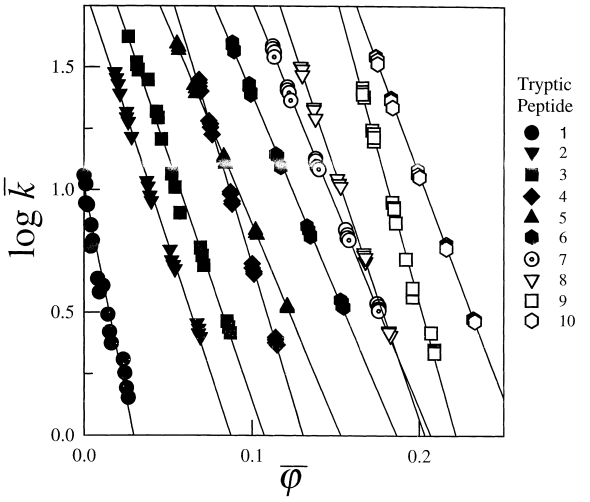

Fig. 5. Plot of retention factor (log $\bar{k}$) versus the mobile phase volume fraction ($\bar{\phi}$) for tryptic peptide fragments of equine cytochrome *c* [with the values of $\bar{k}$ and $\bar{\phi}$ calculated according to linear solvent strength (LSS) theory] derived from five different gradient slopes (5, 10, 20, 40 and 60 min) on Chromolith Performance RP-18e. Intersections of lines represent peak overlapping. See Experimental section for other details.

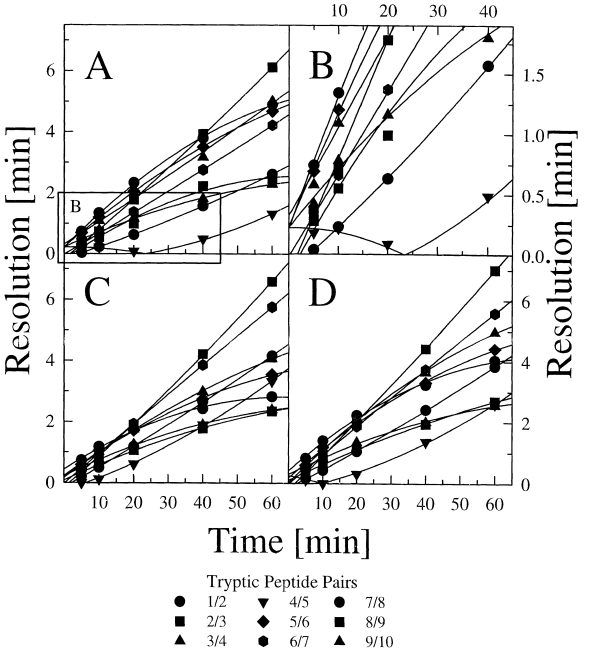

Fig. 6. Relative resolution maps with the resolution R_s versus the gradient run time (all other conditions unchanged) for tryptic peptide fragments of equine cytochrome *c* derived from five different gradient slopes (5, 10, 20, 40 and 60 min) on (A) Chromolith Performance RP-18e, (B) Chromolith Performance RP-18e (enlargement of A), (C) Chromolith SpeedROD RP-18e 50 mm and (D) Chromolith SpeedROD RP-18e 100 mm identifying the respective critical peak pairs and the gradient run-time of maximum resolution. See Experimental section for other details.

3.4. Evaluation of the retention behaviour in terms of solvent strength concepts

As is evident from Figs. 5 and 6 A–D (data shown are for equine cytochrome *c* tryptic digest only although similar data was obtained for the tryptic maps of the other cytochrome *c*s) five different gradient slopes were chosen to generate the log k' versus ϕ plot and the relative resolution maps (RRMs) for all the peptides present in the digest mixture utilising 5, 10, 20, 40 and 60 min gradient run times. These plots allow the appropriate choice of gradient conditions, permitting baseline separation of all the equine cytochrome *c* tryptic peptide fragments (and additionally allowed a sufficiently large elution window in the chromatogram for peptide T5 + T10 to be well resolved from the other peptides in the case of the Gly^{60}-containing cytochrome *c* proteins). In all of these cases application of linear solvent strength concepts was found to inadequately predict the resolution under the separation conditions employed. Consequently, second-order dependencies were investigated with curvilinear fits of the experimental data employed to facilitate evaluation in a biophysical and thermodynamical context of the observed retention behaviour as well as assist in the construction of the relative resolution maps.

The general procedure to obtain RRMs for peptides from data acquired with gradients of different slope or duration via application of linear solvent strength theory has been described elsewhere [2,44–48]. With such RRMs, the resolution versus time curve closest to the abscissa identifies the actual critical peak pair of solutes where the resolution is at a minimum, whilst intersecting curves display transitions between critical peak pairs. Curves intercepting with the abscissa indicate co-elution of the particular peak pair for that separation condition with reversal of the elution order on either side of the intercept (see Fig. 6A–D including Fig. 6B, which is an enlargement of Fig. 6A for additional details). By

identifying local maxima from the area under the curve(s) of the critical peak pair(s), chromatographic conditions suitable for successful separations may be chosen. The RRM for equine cytochrome *c* (Fig. 6B) exhibited a relative maximum at 10 min, the gradient conditions corresponding to the separation shown as Fig. 2A.

From evaluation of the data shown in Fig. 6, it was apparent that all peak pairs exhibit similar behaviour in terms of curvature in the plot of the resolution versus gradient run time on the various silica rod monoliths employed in the study. It thus appears to be an intrinsic feature of monolithic columns that they deliver less selectivity than columns packed with microparticulate sorbents. Smaller values for the respective resolution factors will result but because they can be operated with high flow-rates baseline separations can still be easily achieved for closely eluting peptide solutes with differences in resolution values, $R_s \leq 1$ min. Thus, for fast separations of peptide mixtures, these reversed-phase silica rod monoliths offer the attractive advantage since short gradient times can be employed as part of a method development, such as evident for the separation of all of the tryptic peptides of equine, bovine, canine and avian cytochrome *c*. In this context, the Chromolith Performance RP-18e columns fulfil this demand better than the SpeedROD 50 mm or SpeedROD 100 mm columns. Although these latter columns were designed with the separation of mixtures of organic compounds in mind [49] rather than the separations of complex mixtures of peptides, clearly they still demonstrate some potential for peptide separation. Thus, the shorter SpeedROD 50 mm column displays more robust capabilities in terms of the maintenance of resolution factors as the gradient time or slope was varied. The longer SpeedROD 100 mm column could be exploited to generate very fast separations, e.g., total separation time for the 10 tryptic peptides was less than 4 min (Fig. 7) at a flow-rate of 8 ml/min and gradient time of 4 min based on a local maximum in the RRM (cf. Fig. 6D), although in this latter case baseline separation of all of the equine cytochrome *c* peptides could not be achieved (as evident from the corresponding RRM) due to the steepness of the gradient employed. Similarly, with the tryptic peptides derived from the other cytochrome *c*s the gradient was too steep to permit resolution of peptide T5+T10 from the other late eluting peptide species within the gradient run time.

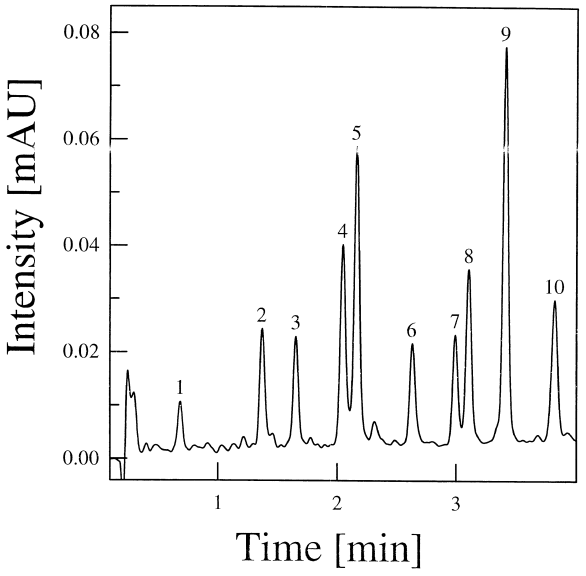

Fig. 7. RP-HPLC separation of tryptic peptide fragments of equine cytochrome *c* on Chromolith SpeedROD RP-18e 100 mm at a gradient run time of 4 min.

3.5. Impact of the influence of structural flexibility of polypeptides or proteins on the resolution behaviour of tryptic peptides using monolithic reversed-phase chromatographic sorbents

Further analysis of the relative resolution maps indicate that the shape of the RRMs can be utilised to investigate structural behaviour of polypeptides in solution and to differentiate between differences in structure when these solutes are adsorbed or in free solution. The nature of the curvature in the RRM may thus be assigned to the state of structural change. Recent studies concerned with the structure of condensed matter involving water [49] and the native and ‘‘molten globule’’ states of proteins in terms of their conformational stability [50] have provided a framework for such evaluations. The structures of crystallised, native and molten globular (MG) states of proteins and large polypeptides differ significantly. The observations presented below are strictly based on the experimental data obtained in

the current series of HPLC investigations and are thus described in qualitative terms pending completion of work in progress in this laboratory related to CD studies, nuclear magnetic resonance (NMR) and Mössbauer spectroscopic investigations.

The crystal structure of a protein, such as cytochrome *c*, can be used to determine the solid state conformations of respective sequence regions that correspond to the peptide fragments prior to enzymatic digestion. The information gained from HPLC studies thus has a direct relevance to an understanding of the role of the MG state(s), which are frequently referred to as intermediate state(s) in protein folding/unfolding. It is well known that the hydrophobic core of many globular proteins is preserved in the MG state, with the generation of compact intermediate state(s) consisting of a significant amount of native-like secondary structures, but with fluctuating tertiary structures [50]. Large polypeptides also can exhibit significant secondary structural propensities in their corresponding MG state(s). In the case of low pH reversed-phase environments with acetonitrile-based eluents, it is known that acetonitrile is an effective solvent for stabilising the α-helical structures of polypeptides [9,10,43,51,52]. Moreover, hydrophobic interactions mediated by the non-polar surface of the sorbent can lead to conformational transitions with globular proteins and polypeptides. As a consequence, amino acid residues that are buried in the native structure of a globular protein can become accessible upon binding of a protein to a sorbent surface containing immobilised *n*-alkyl moieties, or alternatively following enzymatic fragmentation.

An interplay will thus exist between solvent- and ligand-mediated conformational transitions, and these will result in changes in the role of specific amino acids as far as their contribution to the contact binding site. For example, with equine cytochrome *c* the crystal structure of the parent protein indicates [42] that residues Leu^{64} and Leu^{68} do not form part of the accessible surface area. However, in the hydrophobic environment of the reversed-phase ligands, equine cytochrome *c* despite its considerably larger molecular mass and size manifests a retention behaviour that resembles the corresponding peptide fragment T10, which contains both Leu^{64} and Leu^{68}. As noted above, various lines of evidence have suggested that the amino acid sequence corresponding to peptide T10 within the cytochrome *c*s is involved as (part of) the contact binding site of this protein with end-capped *n*-butyl- and *n*-octylsilicas. As the influence of the ligand and solvent are reflected in the corresponding RRM plots, the potential may thus exist that the curvature of these plots, based on the retention behaviour of each individual peptide relative to other peptides in the mixture, contains information related to these molecular events.

Thus, it is noteworthy that the peptide peaks gave rise to two types of curves in the RRMs as they generate peak pairs with their respective neighbours (with the exception of peptide T1 and T10). By evaluating the sign of the curvature of these RRM profiles as the acetonitrile content was increased, structural changes during the course of the elution become evident. This behaviour was exemplified from an evaluation of the retention data acquired under linear gradient conditions for the critical peptide pairs T4/T5 and T7/T8 (Fig. 6A, B), where the curvature of the plots is negative from t equal to zero to the intercept with the abscissa and positive thereafter. By examining the peptide pair T4/T5 with respect to the behaviour of peptide T4 at decreasing gradient steepness, it is apparent that the retention behaviour of peptide T4 approaches that of peptide T5 with decreasing resolution until co-elution occurs. After co-elution the sign of the curvature changes with concomitant increase in the resolution. Is this behaviour of peptide T4 associated with a conformational change or another molecular property? Fragment T5 consists of 5 amino acid residues whereas peptide T4 contains 14 residues. In the X-ray crystallographic structure of equine cytochrome *c* the amino acid sequence corresponding to peptide T4 does not exhibit specific secondary structural preferences and on generation by proteolytic cleavage would be expected to assume a random coil structure. If on the other hand, peptide T4 adopted an amphipathic structure in solution or at the non-polar surface of the monolith sorbents, then amino acid residues Thr^{40}, Ala^{43}, Phe^{46}, Thr^{49} and Asn^{52} would all be on the same face of the molecule. Experimentally, with increasing residence in the stationary phase, the elution of peptide T4 occurs at higher acetonitrile content. This behaviour is con-

sistent with peptide T4 undergoing a conformational change, which favours adsorption as an amphipathic structure due to the cooperative effect promoted by the increase in acetonitrile content (i.e., later elution) that accompanies this phenomenon.

From an examination of the corresponding data for the peptide pair T7/T8 these considerations can be expanded. In this case, the curvature is positive after the intercept with the abscissa. This peptide pair also involves a small (seven amino acid residues) fragment (peptide T7) and a larger (11 amino acid residues) fragment (peptide T8) both of which were formerly not involved in secondary structure elements within the parent cytochrome *c*. Additional information can be gained from the neighbouring peak pairs. Thus, with the peptide pair T6/T7 no curvature was observed in the RRM plot. The amino acid sequence corresponding to peptide T6 (consisting of eight amino acid residues) was involved in an α-helical structure in the parent protein. The linearity of the plot indicating that structural changes with respect to each peptide in this pair are not significant. In contrast, the curvature of the peptide pair T8/T9 was found to be positive indicating that yet again structural variations may have occurred with respect to each peptide in the latter pair.

These findings suggest that all peak pairs comprising structures with an α-helical element (as occurs in the parent protein) display negative curvature possibly due to the helicity enhancing properties of the organic modifier, whereas for sequences previously determined not to be involved in any specific secondary structure in the parent protein, positive curvature is evident for the respective peptide fragment pair in the relative resolution map. In this context, it is noteworthy that investigations concerned with the nature of water structure and hydrophobic interactions have also reported similar dome-shaped free energy effects with proteins and moreover form the basis of different elution patterns of proteins with endcapped and regular RP and hydrophobic interaction chromatography stationary phases. With Lys residues contributing about 34.5% to the accessible surface area in the native cytochrome *c* protein, secondary interactions between the residual silanol groups on the silica surface and the protein have also to be considered. However, in the case of the tryptic fragments, each peptide contains only one basic amino acid residue, so the impact of basic side chain or amino-terminal groups will effectively be common for all of the tryptic fragments and thus peptide–silanol interactions are unlikely to be responsible for the curvature evident in the RRMs and associated retention behaviour.

4. Conclusions

In this investigation, the use of silica rod monoliths has been demonstrated to significantly reduce separation times for peptide map analysis, thus enabling increased sample throughput. Moreover, procedures developed for microparticulate sorbents could be readily transferred to these new stationary phase systems. The reproducibility of the chromatographic profiles enabled the monitoring of sequence variations of protein homologues whilst determination of the putative binding domains could be ascertained from the respective tryptic peptides obtained after digestion. Thus, application of hydrophobicity coefficients and chromatographic profiles have permitted the identification of the molecular nature of the chromatographic contact regions of parent proteins to RP monolithic sorbents utilising foot-printing methods with the contributing peptide fragments. Solvent strength concepts have been utilised to evaluate the obtained data and second order dependencies have been established to enable RRMs corresponding to the observed retention behaviour to be constructed. Analysis of these RRMs within the framework of the structure of condensed matter and conformational stability of protein states can be utilised to investigate the behaviour of these peptides and parent proteins in relation to their chromatographic retention and associated biophysical properties such as conformational transitions upon adsorption to these reversed-phase monolithic sorbents.

Acknowledgements

These investigations were supported by the Australian Research Council. The monoliths were generously provided by Dr. Dieter Lubda and courtesy of

Merck, Darmstadt, Germany. Dr. James Whisstock is thanked for assistance with editing the PDB files.

References

[1] M.I. Aguilar, M.T.W. Hearn, Methods Enzymol. 270 (1996) 1.
[2] R.I. Boysen, M.T.W. Hearn, in: J.E. Coligan, B.M. Dunn, H.L. Ploegh, D.W. Speicher, P.T. Wingfield (Eds.), Current Protocols in Protein Science, Wiley, New York, 2001, p. 1.
[3] W.S. Hancock, C.A. Bishop, R.L. Prestidge, D.R. Harding, M.T.W. Hearn, Science 200 (1978) 1168.
[4] M.T. Hearn, B. Anspach, Bioprocess Technol. 9 (1990) 17.
[5] M.T.W. Hearn, in: S. Ahuja (Ed.), Handbook of Bioseparations, Academic Press, San Diego, 2000, p. 71.
[6] C.T. Mant, R.S. Hodges, Methods Enzymol. 271 (1996) 3.
[7] S.E. Blondelle, R.A. Houghten, Biochemistry 31 (1992) 12688.
[8] R.I. Boysen, A.J.O. Jong, M.T.W. Hearn, Biophys. J. 82 (2002) 2279.
[9] R.I. Boysen, Y. Wang, H.H. Keah, M.T.W. Hearn, Biophys. Chem. 77 (1999) 79.
[10] M.T.W. Hearn, in: M.A. Vijayalakshmi (Ed.), Theory and Practice of Biochromatography, Harwood Academic, 2001.
[11] R.S. Hodges, B.Y. Zhu, N.E. Zhou, C.T. Mant, J. Chromatogr. A 676 (1994) 3.
[12] S.E. Blondelle, E. Perezpaya, G. Allicotti, B. Forood, R.A. Houghten, Biophys. J. 69 (1995) 604.
[13] M.T.W. Hearn, G.L. Zhao, Anal. Chem. 71 (1999) 4874.
[14] E. Lazoura, I. Maidonis, E. Bayer, M.T.W. Hearn, M.I. Aguilar, Biophys. J. 72 (1997) 238.
[15] T.H. Lee, P.E. Thompson, M.T.W. Hearn, M.I. Aguilar, Int. J. Peptide Protein Res. 49 (1997) 394.
[16] S.W. Lin, B.L. Karger, J. Chromatogr. 499 (1990) 89.
[17] P. Oroszlan, S. Wicar, G. Teshima, S.L. Wu, W.S. Hancock, B.L. Karger, Anal. Chem. 64 (1992) 1623.
[18] A.W. Purcell, M.I. Aguilar, M.T.W. Hearn, Anal. Chem. 65 (1993) 3038.
[19] A.W. Purcell, M.I. Aguilar, M.T.W. Hearn, J. Chromatogr. A 711 (1995) 61.
[20] A.W. Purcell, M.I. Aguilar, R.E.H. Wettenhall, M.T.W. Hearn, Pept. Res. 8 (1995) 160.
[21] K.L. Richards, M.I. Aguilar, M.T.W. Hearn, J. Chromatogr. A 676 (1994) 17.
[22] N.E. Zhou, C.T. Mant, R.S. Hodges, Pept. Res. 3 (1990) 8.
[23] M.T.W. Hearn, R. Boysen, Y. Wang, S. Muraledaram, in: Peptide Science: Present and Future, Kluwer Academic Publishers, Dordrecht, Boston, London, 1999, p. 240.
[24] K. Cabrera, D. Lubda, H.M. Eggenweiler, H. Minakuchi, K. Nakanishi, J. High Resolut. Chromatogr. 23 (2000) 93.
[25] K. Cabrera, G. Wieland, D. Lubda, K. Nakanishi, N. Soga, H. Minakuchi, K.K. Unger, Trends Anal. Chem. 17 (1998) 50.
[26] N. Ishizuka, H. Minakuchi, K. Nakanishi, N. Soga, N. Tanaka, J. Chromatogr. A 797 (1998) 133.
[27] H. Minakuchi, K. Nakanishi, N. Soga, N. Ishizuka, N. Tanaka, Anal. Chem. 68 (1996) 3498.
[28] H. Minakuchi, K. Nakanishi, N. Soga, N. Ishizuka, N. Tanaka, J. Chromatogr. A 797 (1998) 121.
[29] M. Schulte, D. Lubda, A. Delp, J. Dingenen, J. High Resolut. Chromatogr. 23 (2000) 100.
[30] P. Zollner, A. Leitner, D. Lubda, K. Cabrera, W. Lindner, Chromatographia 52 (2000) 818.
[31] D. Josic, A. Buchacher, A. Jungbauer, J. Chromatogr. B 752 (2001) 191.
[32] M.I. Aguilar, D.J. Clayton, P. Holt, V. Kronina, R.I. Boysen, A.W. Purcell, M.T.W. Hearn, Anal. Chem. 70 (1998) 5010.
[33] F.E. Regnier, Science 238 (1987) 319.
[34] H.M. Huang, F.Y. Lin, W.Y. Chen, R.C. Ruaan, J. Colloid Interface Sci. 229 (2000) 600.
[35] F.Y. Lin, W.Y. Chen, R.C. Ruaan, H.M. Huang, J. Chromatogr. A 872 (2000) 37.
[36] D. Lubda, Merck, Darmstadt, personal communication.
[37] E. Hoff, R.C. Chloupek, Methods Enzymol. 271 (1996) 51.
[38] I. Molnar, R.I. Boysen, P. Jekow, J. Chromatogr. 485 (1990) 569.
[39] A.J. Round, M.I. Aguilar, M.T. Hearn, J. Chromatogr. A 661 (1994) 61.
[40] M.C.J. Wilce, M.I. Aguilar, M.T.W. Hearn, Anal. Chem. 67 (1995) 1210.
[41] R.I. Boysen, A.J.O. Jong, J.A. Wilce, G.F. King, M.T.W. Hearn, J. Biol. Chem. 277 (2002) 23.
[42] G.W. Bushnell, G.V. Louie, G.D. Brayer, J. Mol. Biol. 214 (1990) 585.
[43] M.A.J. Chowdhury, R.I. Boysen, H. Ihara, M.T.W. Hearn, J. Phys. Chem. B 106 (2002) 11936.
[44] R.I. Boysen, V.A. Erdmann, M.T.W. Hearn, J. Biochem. Biophys. Methods 37 (1998) 69.
[45] B.F.D. Ghrist, L.R. Snyder, J. Chromatogr. 459 (1988) 43.
[46] B.F.D. Ghrist, B.S. Coopermann, L.R. Snyder, J. Chromatogr. 459 (1988) 1.
[47] B.F.D. Ghrist, L.R. Snyder, J. Chromatogr. 459 (1988) 25.
[48] L.R. Snyder, in: Cs. Horvath (Ed.), HPLC—Advances and Perspectives, Academic Press, New York, 1980, p. 208.
[49] I.M. Klotz, J. Phys. Chem. 103 (1999) 5910.
[50] D. Hamada, Y. Kuroda, M. Kataoka, S. Aimoto, T. Yoshimura, Y. Goto, J. Mol. Biol. 256 (1996) 172.
[51] R.I. Boysen, A.J.O. Jong, M.T.W. Hearn, manuscript in preparation.
[52] M.T.W. Hearn, H.H. Keah, R.I. Boysen, I. Messana, F. Misiti, D.V. Rossetti, B. Giardina, M. Castagnola, Anal. Chem. 72 (2000) 1964.